The accuracy of radio direction finding in the Extremely Low Frequency range

Janusz Mlynarczyk[1], Andrzej Kulak[1], and Jacobo Salvador[2]

[1]AGH University of Science and Technology, Department of Electronics, 30-059 Krakow, Poland.

[2]Observatorio Atmosferico de la Patagonia Austral, OAPA UNIDEF (MINDEF - CONICET), Río Gallegos, Argentina.

Corresponding author: Janusz Mlynarczyk (januszm@agh.edu.pl)

Key Points:

- Using a newly installed broadband ELF receiver, we analyzed 1000 strong atmospheric discharges at distances of up to 5000 km
- We identified the most important factors that influence the accuracy of radio direction finding
- Our analytical radio wave propagation model allowed us to explain the obtained results.

Abstract

In this work, we study the accuracy of direction finding in the Extremely Low Frequency (ELF) range using a newly installed broadband receiver equipped with two active magnetic antennas. The main natural source of ELF radio waves is lightning. In this work, we analyzed 1000 atmospheric discharges at distances of up to 5000 km from the receiver. We identified the most important factors influencing the accuracy of the angle of arrival: the deviation of the radio waves propagating through the day-night terminator zone and the signal-to-noise ratio resulting from local electromagnetic noise and Schumann Resonance background. The obtained results clearly show that the accuracy of estimating the direction of arrival is very high (an average error of 0.1° with the standard deviation of 2.3°) when the signal-to-noise ratio is large (the amplitude of the magnetic field component above 100 pT), except for short periods in the local morning and evening, when the day-night terminator is present on the propagation path of the direct wave. For the day-night propagation paths, the refraction angle was larger than the incidence angle, and for the night-day propagation paths, the refraction angle was smaller than the incidence angle, which is consistent with theory. Using our analytical ELF radio propagation model allowed us to explain the obtained results.

1 Introduction

In this work we analyze data from our new ELF receiver equipped with two magnetic antennas, which was set up in Patagonia in southern Argentina. The station was built using our most recent generation of ELF equipment [*Kulak et al.*, 2014]. It features a frequency bandwidth of 0.03 to 300 Hz. It is part of our ongoing project, called the World ELF Radiolocation Array (WERA), the intention of which is to locate the strongest atmospheric discharges occurring anywhere on Earth. One station enables us to find the direction of arrival of the signal. Two stations would allow us to determine the location of the source. The third station would make it possible to increase the accuracy of the location and to determine the polarity of the source.

In this study, we focus on the accuracy of direction finding using one receiver equipped with two orthogonal magnetic antennas (induction coils). In a similar study published recently by *Bor et al.* [2016], the authors analyzed the accuracy of direction finding using their ELF station in Hungary. They identified the local anisotropic ground conductivity as the dominant factor of error. Once identified, it can be minimized using an angle-dependent correction factor. We show that in our case, the main factor influencing accuracy is the presence of the day-night terminator zone and the signal-to-noise ratio. The obtained maximum error in the angle of arrival due to the terminator zone was 12°, which is consistent with the residual bearing deviation found by an early study with a very narrowband systems (4-16 Hz and 4-19 Hz; *Füllekrug and Sukhorukov*, [1999]). However, the mean error in the direction finding and its standard deviation are significantly smaller in our case. This could be related to much broader frequency range of our receiver leading to a smaller influence of local anisotropies on direction finding. Lightning location in the ELF range has also been studied at large distances. *Boccippio et al.* [1998] analyzed 40 events observed from TRMM satellite at the distances of up to 20 Mm and found that the mean ground range error was 2 Mm. Single-station Schumann resonance method has also been used by *Williams et al.* [2007] for a sprite lighting at the distance of 16.6 Mm. *Williams et al.* [2010] analyzed sprites lighting events from Africa detected by several ELF stations worldwide. *Mlynarczyk et al.* [2015] analyzed strong lighting discharges at the distances of up to 12 Mm using two ELF receivers, one located in Poland and the other in Colorado, USA.

Some other studies related to lighting location that the reader might be interested in include *Reising et al.* [1996], and *Fullekrug and Constable* [2002],

In our study, we analyzed 1000 strong lightning discharges at distances of up to 5000 km from the receiver. To our knowledge, this is the first study of radio direction finding performed with a broadband ELF receiver (0.03-300 Hz) on such a large data set. The use of a broadband receiver allowed us to work with impulses that had high amplitude, limiting the influence of Schumann resonance background on the obtained results.

2 Data and Methods

Two orthogonal magnetic antennas enable us to infer the angle of arrival (AoA) of the recorded signal. There are several factors that influence its accuracy. The first one is the accuracy of antenna alignment toward the geographic north and east. We set up the antennas using a liquid-filled compass with a sighting mechanism for precise bearing and the IGRF model [*Thébault et al.*, 2015] to correct for the magnetic declination. To increase the precision of bearing we used long cords fixed to ground stakes, which we aligned with the geographical north-south and east-west directions and with the two antennas. We recheck the alignment using another liquid-filled compass and an electronic compass. We also checked the length of hypotenuse of a triangle formed by the stakes and cords. This way both the correct direction and the 90° angle between the two antennas were checked. However, the accuracy of this procedure is still limited; we did not expect it to be better than about ±1°. Another factor that can influence the angle of arrival inferred from the signal is the local ground conductivity [*Bor et al.*, 2016]. The accuracy of direction finding is also strongly influenced by the Schumann Resonance background. To limit its influence, for this analysis we chose the signals that had the amplitude of at least 100 pT. Due to very low attenuation of ELF waves and a wide bandwidth of our receiver, we typically record a few hundred discharges per hour which meet this criterion. In this study, we excluded sources located farther than 5000 km from the receiver in order to exclude any additional effects that might be related to long range propagation, rather than the direction finding itself.

Most atmospheric discharges take the form of short impulses (Figure 1).

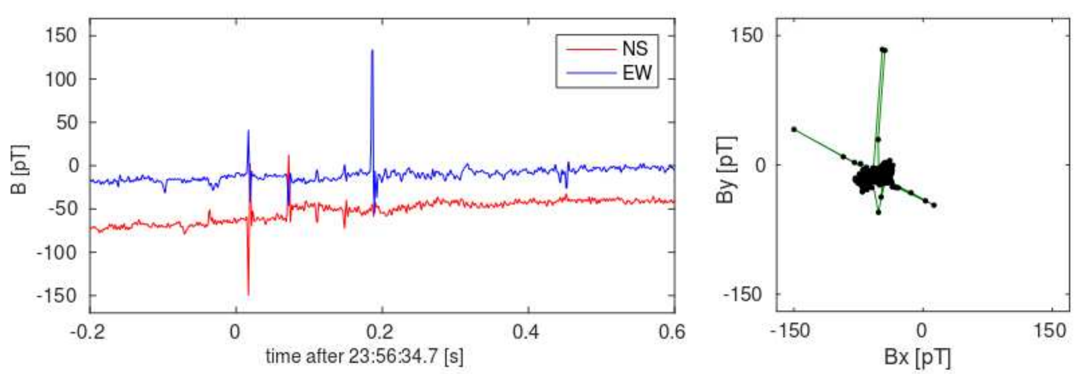

Fig. 1. Atmospheric discharges recorded by two orthogonal magnetic antennas, north-south (NS) and east-west (EW) on 28 March 2016 (left panel). NS versus EW component for the same time segment (right panel).

The simplest way to infer the angle of arrival is to take the ratio of the peak amplitudes recorded by the two magnetic antennas and calculate the inverse tangent. Another method would be to perform digital antenna rotation in software until the maximum is found in one channel and zero in the other channel, but this method is more difficult to automate. We will illustrate this in section 3.

Figure 2 shows a typical spectrum recorded by our ELF receiver, in which we identified three main sources that have negative influence on the accuracy of direction finding: power line noise, Schumann Resonance background and 1/f noise. The Schumann Resonance background exhibits diurnal, seasonal and geographical variability, due to its dependence from the intensity and location of storm centers. Therefore, the signal-to-noise ratio will also exhibit such variability [*Huang et al.*, 1999].

The accuracy of direction finding can be improved significantly by reducing 1/f noise, which include both geophysical and instrumental contributions. Therefore, we used a high pass filter with a cutoff frequency of 2 Hz. The chosen cutoff frequency is a tradeoff between the accuracy of direction finding and ELF waveform distortions that a high pass filter can cause. We also removed the 50 Hz power line noise and its third harmonic. We used a third order bandstop digital Butterworth filter with the bandwidth of 0.4 Hz. Interestingly enough, a 60 Hz power line noise is sometimes visible in our spectra (see Figure 2), even though the closest 60 Hz power grid system is located about 2500 km away.

The sampling rate of the station is 887.784 Hz. In order to find more accurately the peak amplitude, we resample the signal at 5 times the original sample rate. Resampling consists in inserting additional samples between each of the original samples [*Proakis and Manolakis,* 2007, chapter 6], and it can be treated as an interpolation. The obtained waveform is smoother and the peak amplitude (as well as the timing) can be read with better precision.

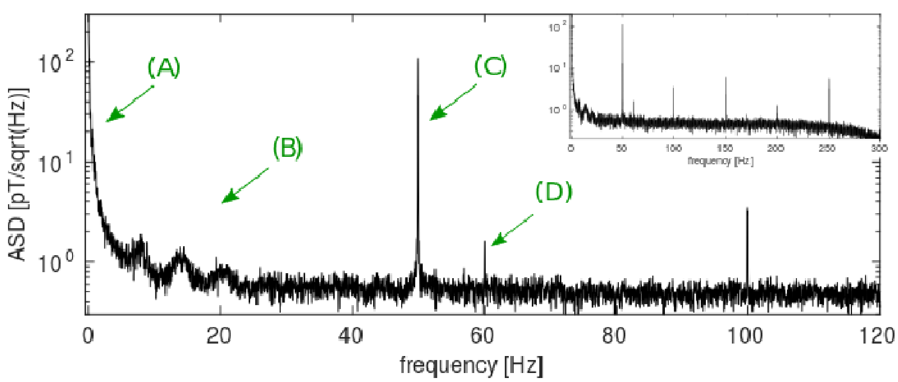

Fig. 2. A typical spectrum obtained from a five-minute recording (27 March 2016, 2:15 UT). Three factors limiting the direction finding accuracy can be seen: **(A)** 1/f noise (increase in geophysical and instrumental noise as the frequency decreases); **(B)** Schumann Resonance background (three maxima can be clearly seen: around 8, 14 and 20 Hz); **(C)** power line noise at 50 Hz; **(D)** sporadically present 60 Hz power line noise. **(top right corner)** Spectrum view up to 300 Hz, with clearly visible power line harmonic frequencies at 100, 150, 200 and 250 Hz.

All the discharges were identified using data from the WWLLN lightning detection network [*Rodger et al.*, 2006] and taking into account the time of arrival (ToA). The reported location was used as a reference for determining the error in the angle of arrival (AoA). We defined this error as the difference between the azimuth inferred from the location reported by WWLLN and the azimuth obtained from the ELF data. The WWLLN network operates in the

Very Low Frequency (VLF, 3-30 kHz) band, and its ultimate aim is to provide location of cloud-to-ground (CG) discharges with mean location accuracy below 10 km [*Rodger et al.*, 2006]. As of 2012 [Hutchins *et al.*, 2012], WWLLN consisted of 60 stations distributed around the world. The detection efficiency was estimated to be of about 11% for cloud-to-ground (CG) strokes and above 30% for higher peak current flashes over the Continental United States. The WWLLN located 61% of strokes with the accuracy of below 5 km [Hutchins *et al.*, 2012].

3 Results and discussion

We analyzed 1000 impulses with an amplitude of above 100 pT and which originated from cloud-to-ground discharges detected by WWLLN between March 27 and April 6, 2017. To obtain such long data span we set the WWLLN energy threshold to 50 kJ. This allowed us to reduce the number of empty angles (directions without any lightning). Figure 3 shows the location of the discharges.

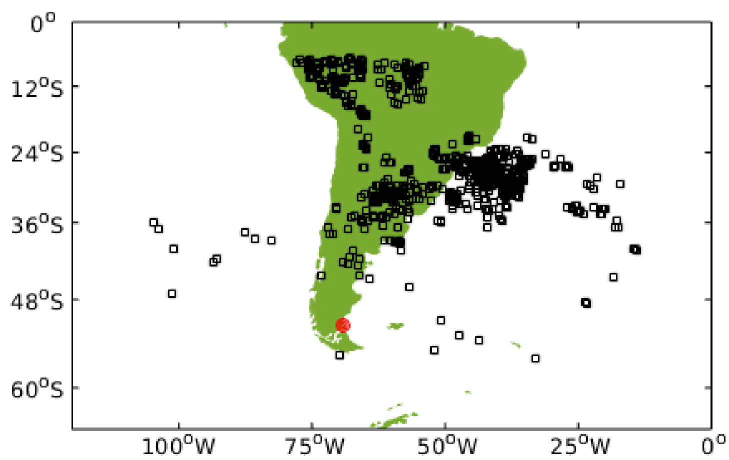

Fig. 3. Location of the lightning discharges considered in this study (black squares; provided by WWLLN) and location of the Patagonia ELF station (red circle). (Data visualized using M_Map mapping package.)

Figure 4 presents the error in the direction of arrival at various hours of the day for discharges at distances of up to 3500 km (top panel) and 5000 km (bottom panel).

We can see two periods during the day where the error is clearly higher. These are periods during which the day-night terminator is above South America. Figure 5 shows the terminator's location at 10:00 and 22:00 UTC.

At around 10:00 UTC the error was positive, which means that the azimuth calculated from the WWLLN data was larger than the azimuth estimated from the ELF recording. At around 22:00 UTC the error was mostly negative, which means that the azimuth obtained from the WWLLN data was smaller than the azimuth inferred from the ELF signal.

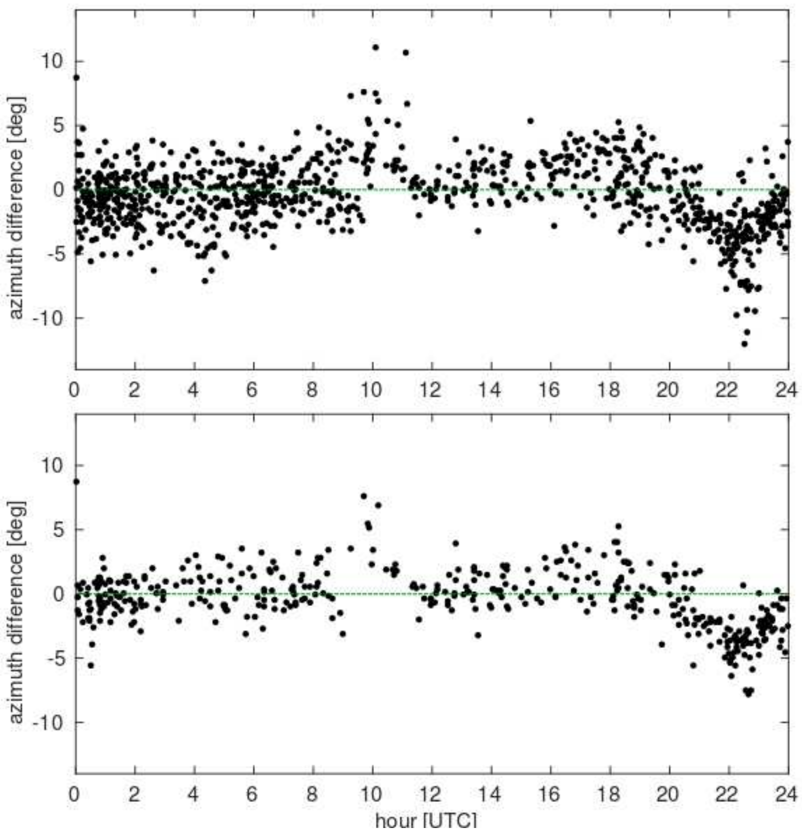

Fig. 4. The error in the azimuth estimation from the ELF recording based on the location reported by the WWLLN lighting detection network. **(top)** Discharges at distances of up to 3500 km. **(bottom)** The entire data set considered in this study (distances of up to 5000 km). Two periods during the day where the error is clearly higher coincide with the presence of day-night terminator above South America (see Figure 5).

Fig. 5. Day and night zones and the location of the day-night terminator (astronomical, nautical and civil shown in various shades of gray, from darker to lighter, respectively) at 10 UT (left panel) and 22 UT (right panel) on April 5, 2016. The red circle shows the receiver location. Day and night maps courtesy of www.timeanddate.com.

To understand these results, we assume a sharp boundary between the day and night zones and use the Snell's law [*Davis*, 1990, p. 73]. The phase velocities in the day and night time zones are related to the sines of the angles of incidence θ_1 and refraction θ_2:

$$v_{night}\sin\theta_1 = v_{day}\sin\theta_2. \quad (1)$$

The refraction principle on the day-night path is illustrated in Figure 6.

The phase velocity in the Earth-ionosphere waveguide can be calculated from [*Mushtak and Williams*, 2002]

$$v(f) = \frac{c}{\mathrm{Re}\,\bar{S}(f)}, \quad (2)$$

where $\bar{S}$ is the dimensionless frequency dependent complex propagation parameter, which is related to the wave number $\bar{k}$ by the equation [*Kulak et al.*, 2013]:

$$\bar{S} = \frac{c}{\omega}\bar{k}. \quad (3)$$

The propagation parameter $\bar{S}$ can be calculated from [*Mushtak and Williams*, 2002]

$$\bar{S}(f)^2 = \frac{\bar{h}_m(f)}{\bar{h}_e(f)}, \quad (4)$$

where $\bar{h}_m$ and $\bar{h}_e$ are the complex magnetic and electric altitudes of the Earth-ionosphere waveguide, and they are frequency dependent [*Kulak and Mlynarczyk*, 2013].

From our ELF propagation model [*Kulak and Mlynarczyk*, 2013], we obtained the complex altitudes and then calculated the phase velocities for the day and night propagation paths. Since the deviation of the trajectory was based on the peak amplitude comparison, we were interested in the phase velocity at the frequency close to the upper cut-off frequency of the receiver. We got the following values at 300 Hz:

$$v_{day} = 0.823\,c \quad (4)$$

$$v_{night} = 0.944\,c \quad (5)$$

First, we analyze the radio wave propagation from the dayside to the night side (Fig. 6). Let's assume a long propagation distance, for example, $d = 4800$ km, and a large refraction angle, $\theta_2 = 80^\circ$, which should generate a large error. The angle of arrival at the ELF receiver location for this case is about 10° (assuming for simplicity that the terminator is a sharp boundary along the meridian located in the middle of the propagation path). Using (1) we obtain:

$$\sin\theta_1 = v_{day}\sin\theta_2 / v_{night} = 0.856,$$

which gives the incidence angle $\theta_1 = 59^\circ$. Once θ_1 and θ_2 are known, we can calculate the error in the direction of arrival based on the geometry of the propagation path (as seen in Fig. 6)

$$\Delta = Az_{Source} - Az_{ELF} = 10.5^\circ$$

The obtained error in the direction of arrival is positive, which means that the azimuth to the source location Az_{Source} is larger than the azimuth inferred from the ELF data Az_{ELF}. Taking a very small refraction angle, for example 10°, which means that the angle of arrival is 80°, we obtain the incidence angle of 8.7° and the error in the angle of arrival

$$\Delta = Az_{Source} - Az_{ELF} = 0.65^{o}$$

Taking the refraction angle of 45°, we obtain the incidence angle of 38.1° and the error in the angle of arrival

$$\Delta = Az_{Source} - Az_{ELF} = 3.5^{o}$$

For the propagation from the night side to the dayside, we obtain negative values. For example, for the angle of arrival of 45°, we obtain the incidence angle of 54.2° and the error in the angle of arrival

$$\Delta = Az_{Source} - Az_{ELF} = -4.6^{o}$$

The obtained results provide a very good explanation for the errors shown in Figure 4. Since most discharges were located north-east of the receiver location, the radio waves propagated mostly on the day-night paths around 10 UT, generating positive errors, and mostly on the night-day paths around 22 UT, causing negative errors. As a result, the average error obtained with the whole data set is very small.

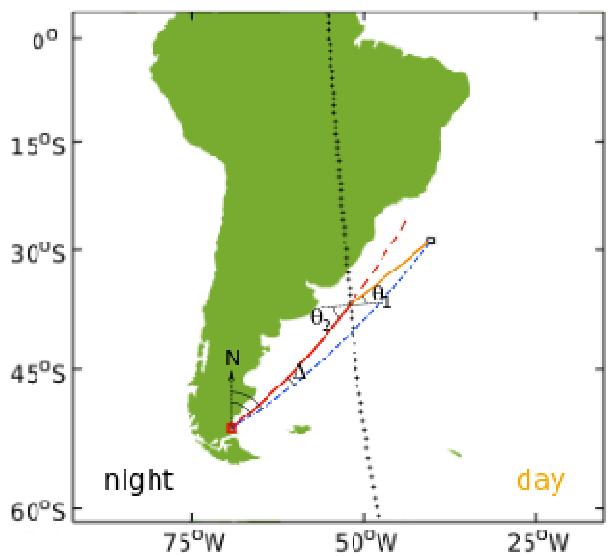

Fig. 6. Illustration of refraction principle on a day-night path. The discharge is located on the dayside (black square) and the receiver is on the night side (red square). The propagation path between the source and the boundary is shown by the orange line. At the day-night boundary the direction changes due to refraction and follows the red line. Therefore, the direction of arrival inferred from the ELF signal is consistent with the red line, which is the source of error.

Table 1 shows the average error in the direction of arrival and its standard deviation for the whole data set, as well as for two subsets. In the first subset of data, we excluded discharges occurring at distances longer than 3500 km. In the second subset, we excluded two hours in the local morning and evening, when the day-night terminator has the largest influence on the radio wave propagation. The residual error is very small, which proves that the antennas were positioned accurately (at the distance of 5000 km, the mean error of 0.4° is equivalent to about 32 km, and 0.1° is equivalent to about 8 km).

Table 1. Average error and standard deviation obtained by the comparison between the direction of arrival based on WWLLN and that calculated from the ELF recordings.

Maximum distance from the source	Average error in the angle of arrival (AoA)	Standard deviation	Comments
5000 km	-0.4°	2.6°	1000 discharges
3500 km	-0.4°	2.3°	429 discharges
5000 km	-0.1°	2.1°	850 discharges; excluding two hours with the largest influence of the terminator in the morning and in the evening.

Figure 7 shows the impulses with the largest positive (top) and negative (bottom) errors in the calculated direction of arrival. It can be seen that the signal-to-noise ratio was good in both cases. Therefore, we can conclude that the main contribution to the error was from propagation through the day-night terminator zone.

Since the discharge location is known and the signal was recorded by horizontal magnetic antennas, the knowledge of the phase relationship between the coils and use of Ampere's Law enable us to infer the polarity of the vertical current source. In the first case (top panel in Figure 7), the source had a positive polarity (a positive cloud-to-ground discharge, +CG). In the second case (bottom panel in Fig. 7), the source had a negative polarity (negative cloud-to-ground discharge).

Both impulses shown in Figure 7 are delayed by about 21 ms from the timing reported by WWLLN. The reason for this is the propagation delay and the receiver delay. Our propagation model [*Kulak and Mlynarczyk,* 2013] and method [*Mlynarczyk et al.*, 2015] allow us to reconstruct the current moment waveform at the source location. The timing at the source should agree with the WWLLN reported time. We illustrate this for the impulse shown in the top panel in Figure 7.

The first step consists of digital antenna rotation [*Mlynarczyk et al.*, 2015]. Figure 8 shows the impulse after antenna rotation by 8.8°, which is the angle of arrival found by the comparison of peak amplitudes in both channels. As a result, the antennas are digitally aligned to the direction of arrival (one is parallel and the other perpendicular). Therefore, the blue plot represents the azimuthal magnetic field component. The other antenna is orthogonal, so the amplitude in the other channel is zero during the peak (or close to zero, due to noise). The same procedure can be applied to the second impulse.

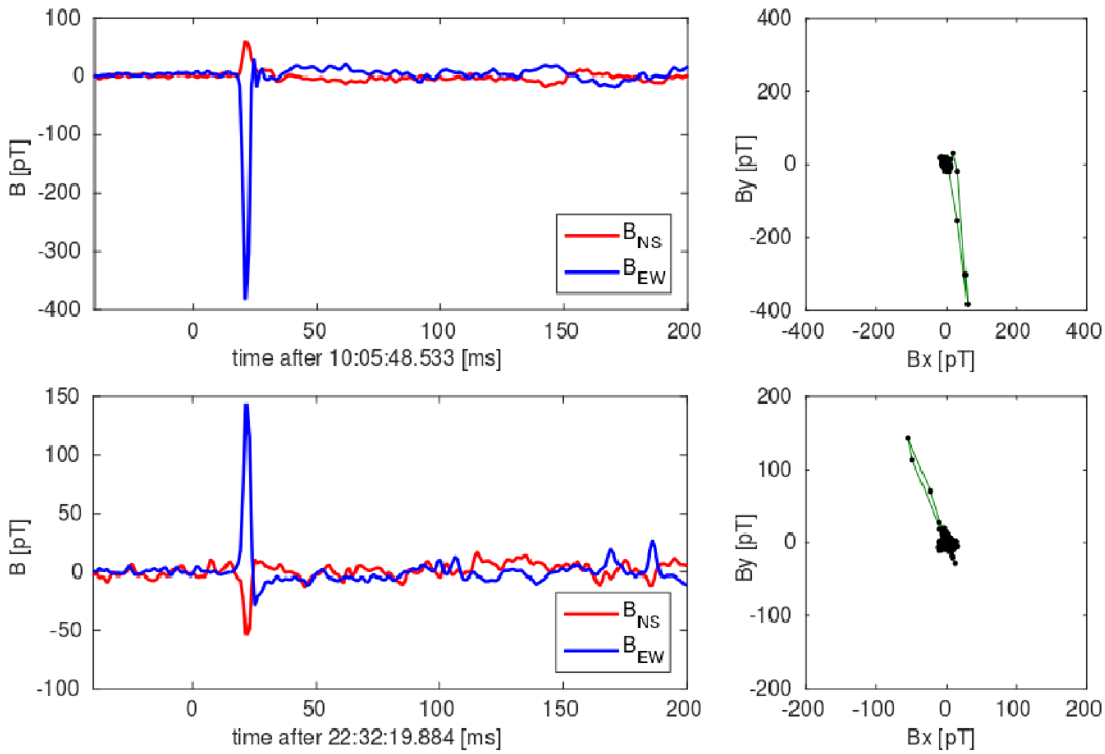

Fig. 7. Signals with the largest positive and negative errors in the angle of arrival. **(top)** Positive cloud-to-ground discharge recorded at 10:06 UT on 30 March 2016. **(bottom)** Negative cloud-to-ground discharge recorded at 22:30 on 5 April 2016. The time axis is relative to the time reported by WWLLN. The ELF propagation delay was not subtracted yet.

To obtain the current moment waveform at the source, we have to find the relationship between the magnetic field component of the electromagnetic wave and the spectral density of the source current moment $\bar{s}(f)$. Such a relationship can be found, for example, in *Porrat et al.* [2001], *Mushtak and Williams* [2002], *Fullekrug et al.* [2006], and *Kulak et al.* [2013]. In this work we use the latter. It was obtained by an analytical solution to Maxwell equations for a vertical electric dipole placed in the Earth-ionosphere waveguide. The magnetic field component of electromagnetic wave recorded at the distance *r* is given by:

$$\bar{B}(r,f) \approx -i\frac{\pi\mu_0 f}{2h_m(f)v(f)} H_1^{(2)}\left(2\pi r\frac{f}{v(f)}\right) e^{-\alpha(f)\,r}\,\bar{s}(f)\bar{g}(f) \qquad [\mathrm{T}] \qquad (6)$$

where f is the frequency, $i=\sqrt{-1}$, μ_0 is the permeability of free space, $h_m(f)$ is the magnetic height of the Earth-ionosphere waveguide, $v(f)$ is the phase velocity, $H_1^{(2)}$ is the Hankel function of the second kind and first order, $\alpha(f)$ is the attenuation rate, $\bar{g}(f)$ is the transfer function of the receiver.

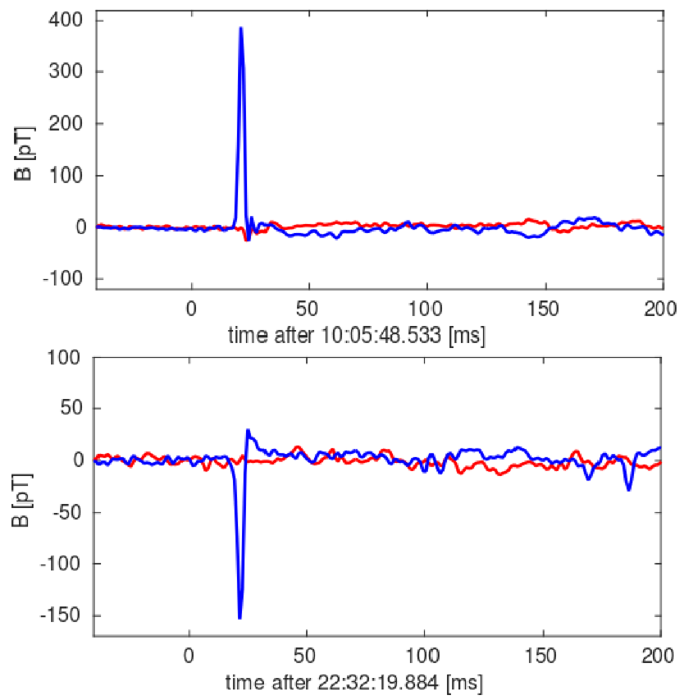

Fig. 8. Azimuthal magnetic field component (blue plot) obtained from the recorded signals shown in Fig. 7, by digitally rotating the antennas towards the direction of arrival. As a result, the impulse polarity is the same as the discharge polarity (that is positive for the discharge shown in top panel and negative for the discharge in the bottom panel).

Processing the signal in the frequency domain, we obtain $\bar{s}(f)$ from (6). Then we return it to the time domain using the inverse discrete Fourier transform (IDFT), obtaining the current moment waveform $s(t)$. We can write it in the following way:

$$\bar{s}(f) \approx \frac{\bar{B}(r,f)}{-i\,\dfrac{\pi\mu_0 f}{2h_m(f)\,v(f)}\,\phi(r)\,H_1^{(2)}\!\left(2\pi r\dfrac{f}{v(f)}\right)e^{-\alpha(f)\,r}\,\bar{g}(f)}; \qquad s(t) = IDFT\left[\,\bar{s}(f)\right] \qquad (7)$$

Since both the radio wave propagation and the receiver are included in the equation, the delay that they introduce is automatically subtracted.

Figure 9 shows the reconstructed current moment waveform. It can be seen that the time at the source agrees with WWLLN reported time. The delay of the signal in this case was 19 ms.

Returning to the analysis of the whole data set, we will show another factor with an influence on the direction finding in the ELF range. As shown in Figure 10, the signal amplitude has a very high influence on the accuracy of the angle of arrival. This is because it determines the signal-to-noise ratio. This is especially clear when sources at distances greater than 3500 km are excluded, which limits the number of cases for which the wave had to propagate through the terminator zone, from the dayside to the night side.

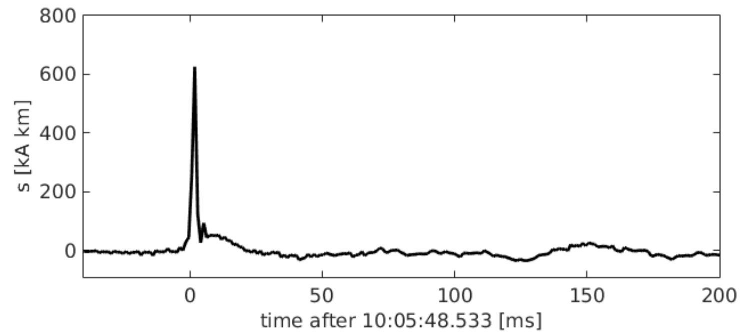

Fig. 9. Current moment waveform of the discharge shown in top panel of Figure 4.

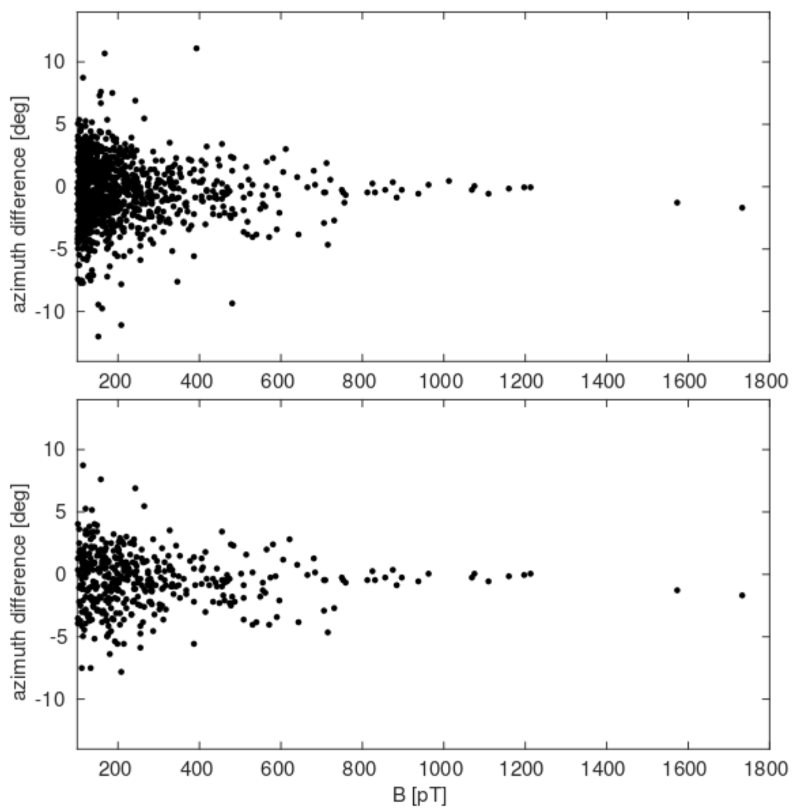

Fig. 10. The error in the calculated direction of arrival versus the peak amplitude of the signal. **(top)** The entire data set. **(bottom)** Distances of up to 3500 km.

4 Summary and conclusions

In this paper, we studied ELF radio wave propagation at distances of up to 5000 km. We analyzed 1000 strong lightning discharges. We calculated the angle of arrival at our ELF station and compared it with the azimuth obtained from the WWLLN lighting location network, which works in the VLF band. We clearly identified two factors that most influence the accuracy of the angle of arrival inferred from our ELF receiver: the signal-to-noise ratio (SNR) and the presence of the day-night terminator.

The accuracy of the direction of arrival was high when the signal-to-noise ratio was large and the day-night terminator was not present on the propagation path (mean error of 0.1°). During short periods in local morning and evening hours, when the terminator was present, the error in the direction of arrival was clearly higher. The maximum error due to propagation through the day-night terminator zone was 12° but the average error was much smaller (-1.9°). It was mostly positive in the morning (the azimuth to the location of the source was larger than the azimuth to the apparent location inferred from the ELF data) and negative in the evening. This translated into larger refraction angles than incidence angles for the day-night propagation paths, and smaller refraction angles than incident angles for the night-day propagation paths. Some basic propagation formulas and our analytical ELF radio wave propagation model allowed us to understand the obtained results.

Acknowledgments

The authors would like to thank Dr. Eduardo J. Quel, Dr. Gabriela Nicora, Jonathan Quiroga and Nahuel Diaz for making the setup of the ELF station possible, as well as the members of the Krakow ELF team for their contribution to the ELF station setup and measurements. The authors wish to thank the World Wide Lightning Location Network (http://wwlln.net), a collaboration among over 50 universities and institutions, for providing the lightning location data used in this paper. The authors would also want to thank the reviewers for useful comments and suggestions. This work has been supported by the National Science Center under Grant 2015/19/B/ST10/01055. The data used to produce the results in this paper are available upon request from the corresponding author.

References

Bór, J., B. Ludván, N. Attila, and P. Steinbach, Systematic deviations in source direction estimates of Q-bursts recorded at Nagycenk, Hungary (2016), *J. Geophys. Res. Atmos.*, 121, doi:10.1002/2015JD024712.

Boccippio, D. J., C. Wong, E. R. Williams, R. Boldi, H. J. Christian, and S. J. Goodman (1998), Global validation of single-station Schumann resonance lightning location, J. Atmos. Sol. Terr. Phys., 60, 701 – 712.

Davis, K., *Ionospheric Radio*, Peter Peregrinus Ltd., 1990.

Füllekrug, M., and A. I. Sukhorukov (1999), The contribution of anisotropic conductivity in the ionosphere to lightning flash bearing deviations in the ELF/ULF range, *Geophys. Res. Lett*., 26(8), 1109–1112, doi:10.1029/1999GL900174.

Fuellekrug, M. and S. Constable (2000), Global triangulation of intense lightning discharges, *Geophysical Res. Let.*, 27, 333-336.

Huang, E., E. Williams, R. Boldi, S. Heckman, W. Lyons, M. Taylor, T. Nelson, and C. Wong (1999), Criteria for sprites and elves based on Schumann resonance observations, J. Geophys. Res., 104, 16,943–16,964, doi:10.1029/1999JD900139.

Hutchins, M. L., R. H. Holzworth, J. B. Brundell, and C. J. Rodger (2012), Relative detection efficiency of the World Wide Lightning Location Network, Radio Sci., 47, RS6005, doi:10.1029/2012RS005049.

Kulak, A., J. Kubisz, S. Klucjasz, A. Michalec, J. Mlynarczyk, Z. Nieckarz, M. Ostrowski, and S. Zieba (2014), Extremely low frequency electromagnetic field measurements at the Hylaty station and methodology of signal analysis, *Radio Sci.*, 49, 361–370, doi:10.1002/2014RS005400.

Kulak, A., J. Młynarczyk, and J. Kozakiewicz (2013), An analytical model of ELF radiowave propagation in ground-ionosphere waveguides with a multilayered ground, *IEEE Trans. Antennas Propag.*, 61(9), 4803–4809, doi:10.1109/TAP.2013.2268244

Kulak, A., and J. Mlynarczyk (2013), ELF propagation parameters for the ground-ionosphere waveguide with finite ground conductivity, *IEEE Trans. Antennas Propag.*, 61(4), 2269–2275, doi: 10.1109/TAP.2012.2227445

Mlynarczyk, J., J. Bór, A. Kulak, M. Popek, and J. Kubisz (2015), An unusual sequence of sprites followed by a secondary TLE: An analysis of ELF radio measurements and optical observations, *J. Geophys. Res. Space Physics*, 120, 2241–2254, doi:10.1002/2014JA020780.

Mlynarczyk J, A. Kulak A and J. Kubisz (2016), Proc. of the 21st Int. Conf. on Microwave, Radar and Wireless Communications (MIKON), IEEE, https://doi.org/10.1109/MIKON.2016.7492093

Mushtak, V. C., and E. R. Williams (2002), ELF propagation parameters for uniform models of the Earth-ionosphere waveguide, *Journal of Atmospheric and Solar-Terrestrial Physics*, 64, pp.1989-2001.

Proakis J. G. and D. G. Manolakis, *Digital Signal Processing: Principles, Algorithms, and Applications*, 4th ed., Chap. 6., Prentice Hall, 2007.

Reising, S. C., U. S. Inan, T. F. Bell, and W. A. Lyons, Evidence for continuing current in sprite-producing cloud-to-ground lightning*, Geophys. Res. Lett.*, 23, 3639, 1997.

Rodger, C. J., S. Werner, J. B. Brundell, E. H. Lay, N. R. Thomson, R. H. Holzworth, and R. L. Dowden (2006), Detection efficiency of the VLF World Wide Lightning Location Network (WWLLN): Initial case study, *Ann. Geophys.,* 24, 3197, doi:10.5194/angeo-24-3197-2006.

Thébault, E., C. C. Finlay, C. D. Beggan, P. Alken, J. Aubert et al. (2015), International Geomagnetic Reference Field: the 12th generation, *Earth, Planets and Space*, 67 (1), doi:10.1186/s40623-015-0228-9.

Williams, E. R., V. C. Mushtak, R. Boldi, R. L. Dowden, and Z.-I. Kawasaki (2007), Sprite lightning heard round the world by Schumann resonance methods. Radio Sci. 42: RS2S20, doi: 10.1029/2006RS003498.

Williams, E. R., W. A. Lyons, Y. Hobara, V. C. Mushtak, N. Asencio, R. Boldi, J. Bor, S. A. Cummer, E. Greenberg, M. Hayakawa, R. H. Holzworth, V. Kotroni, J. Li, C. Morales, T. E. Nelson, C. Price, B. Russell, M. Sato, G. Satori, K. Shirahata, Y. Takahashi, K. Yamashita (2010), Ground-based detection of sprites and their parent lightning flashes over Africa during the 2006 AMMA campaign. Q J R Meteorol. Soc., 136, 257-271, http://doi:10.1002/qj.489, 2010.